Journal of Power Sources 195 (2010) 4119–4123

Contents lists available at ScienceDirect

Journal of Power Sources

journal homepage: www.elsevier.com/locate/jpowsour

Short communication

In situ spectroelectrochemical measurements during the electro-oxidation of ethanol on WC-supported Pt-black, based on sum-frequency generation spectroscopy

Benedetto Bozzini[a,*], Gian Pietro De Gaudenzi[b], Bertrand Busson[c], Christophe Humbert[c], Catherine Six[c], Audrey Gayral[c], Abderrahmane Tadjeddine[d]

[a] Dipartimento di Ingegneria dell'Innovazione, Universita' del Salento, Via Monteroni, I-73100 Lecce, Italy
[b] Films S.p.a., v. Megolo 2, I-28877 Anzola d'Ossola, Italy
[c] Laboratoire de Chimie Physique, Bat 201P2, Univ. Paris-Sud, CNRS, 91405 Orsay, France
[d] UDIL, Bat. 201P1, CNRS, Univ. Paris-Sud, BP 34, 91898 Orsay, France

ARTICLE INFO

Article history:
Received 21 July 2009
Received in revised form 4 January 2010
Accepted 5 January 2010
Available online 18 January 2010

Keywords:
SFG
Electrocatalysis
WC
Pt
Ethanol

ABSTRACT

In this paper we report in situ sum-frequency generation (SFG) spectroscopy experiments, carried out during the electro-oxidation of ethanol on Pt-black supported on tungsten carbide (WC). Well-defined SFG resonances were measured in the 1320–1350 cm^{-1} spectral range with the VIS beam set at 523.5 nm. The assignment of SFG bands was carried out with the aid of vibrational spectra calculated in the framework of Density Functional Theory (DFT). The spectra recorded in situ showed various kinds of changes in terms of spectral patterns and peak intensities, as a function of the applied potential and of the oxidation time, yielding information on the modification of the catalyst-adsorbate structure. To the best of the authors' knowledge, this is the first in situ electrochemical SFG work carried out in this particular wavelength range – specially diagnostic for electrocatalysis and made accessible by use of the CLIO IR free-electron laser – and with an electrode functionalised with a real catalyst, in powder form.
© 2010 Elsevier B.V. All rights reserved.

1. Introduction

The development of proton-exchange membrane fuel cells (PEMFCs) for power generation has brought about new challenges related to the durability of materials. Among them, the degradation of the widely used carbon-supported Pt-based catalysts is becoming a key point that calls for the introduction of alternative materials, with improved long-term resistance to catalyst agglomeration and support corrosion, in addition to the more extensively investigated poison-tolerance. Being characterised by good electronic conductivity, resistance to acidic environment, low cost and outstanding mechanical properties – in addition to some degree of electrocatalytic behaviour towards hydrogen oxidation – tungsten carbide (WC) has been recently indicated as a possible candidate to replace the traditional carbon support [1–10]. CO poisoning during the electro-oxidation of hydrogen at WC was studied in [1] and found to be limited and reversible. Furthermore, the addition of WC to Pt [2], Pt–Ru [2], Pd [8,10] and AuPd [9] catalysis to improve the tolerance to CO during ethanol oxidation, has been proved. The prospective combination of WC with metals not belonging to the platinum metal group has been pointed out as appealing for economical consideration: improved catalytic behaviour was found for nanocrystalline WC, as such and in combination with Ag [3]. Furthermore, the combination of WC with CNT has proved effective in enhancing the activity in Pt–WC electrocatalysts for ethanol oxidation in alkaline media [10].

As far as thermal and electrochemical stability are concerned, a comparative study on WC- and C-supported Pt was carried out in [4]. The two supports were loaded with comparable amount of Pt and subjected to several oxidation cycles: WC was found to be more stable than commercial carbon supports. Moreover, it is worth noting that Pt–WC and Pt–WC/C have been proposed as cathodic catalysts for oxygen reduction [7] and hydrogen production by methanol electrolysis [8].

As a first approach to spectroelectrochemical investigations of WC-supported catalysts, in this work we study the behaviour of WC-supported Pt-black during the prolonged electro-oxidation of ethanol. In subsequent papers, we shall report in situ FTIR and SFG results on catalysts obtained by electrodepositing Pt nanoparticles onto WC. The present research is based on the use of SFG spectroscopy that – due to its extreme sensitivity to the electrochemical interface and its capability of conveying simultaneously vibrational and electronic information – is ideal for the

* Corresponding author. Tel.: +39 0832 297323; fax: +39 0832 297323.
E-mail addresses: benedetto.bozzini@unile.it, benedetto.bozzini@unisalento.it (B. Bozzini).

0378-7753/$ – see front matter © 2010 Elsevier B.V. All rights reserved.
doi:10.1016/j.jpowsour.2010.01.017

identification of support-catalyst modifications under prolonged usage. The authors are not aware of previous in situ electrochemical SFG experiments carried out with actual catalysts in powder form: all cognate experiments have in fact been performed on different faces of Pt single-crystal electrodes.

2. Materials and methods

2.1. Electrode preparation

The catalyst layer was prepared according to the procedure described in [11]: an ink composed of 0.2 g of Pt-black (Aldrich), 0.7 g of Nafion (Aldrich) solution and 4 mL of isopropyl alcohol was sonicated for 1 h. A few drops were cast on the surface of a polished WC electrode and dried under N_2 flow.

2.2. Electrolyte

The composition of the solution employed in our work was: 0.1 M EtOH (Aldrich), 0.1 M $HClO_4$ (Fluka). All the solutions were prepared from analytical grade reagents and Millipore water with resistivity > 18 MΩ cm.

2.3. Spectroelectrochemical methods

SFG spectra were collected in the potential range +0.90 to −1.35 V RHE. A detailed description of the CLIO free-electron laser (FEL)-based SFG setup used for our experiments can be found in [12]. Briefly, a YLF laser source (HighQ Laser) delivers 7 ps pulses at 1047 nm with a 62.5 MHz repetition rate. These pulses form 2 μs long trains with a 25 Hz repetition rate. After amplification, the YLF pulses are used to pump a BBO crystal to produce the 523.5 nm light (around 3 μJ per pulse). To have access to high IR wavelengths with sufficient power to generate non-linear effects, we make use of the CLIO FEL, ranging from 5 to 150 μm, with the same temporal features at the microsecond scale but delivering 1 ps pulses of 10 μJ energy. The FEL is temporally synchronized with the YLF laser source. The spectral resolution of the system in the infrared is about 5 cm^{-1}. The CLIO IR and 523.5 nm laser beams are then spatially (angles of incidence 55° and 65° for the visible and IR beams, respectively) and temporally overlapped at the surface of the working electrode to produce SFG photons ($\mathbf{k}_{SFG} = \mathbf{k}_{Vis} + \mathbf{k}_{IR}$, $\omega_{SFG} = \omega_{Vis} + \omega_{IR}$), detected by photomultipliers after spatial and spectral filtering through a spectrometer. All beams are p-polarised (ppp configuration). All spectra are normalized to their reference spectrum, recorded in parallel in the bulk of a ZnS crystal, in order to get rid of the roto-vibrational absorption by atmospheric water and of laser fluctuations. The spectroelectrochemical cell consists of a Teflon body, closed by a CaF_2 prism and filled with electrolyte, deaerated by Ar bubbling. A three-electrode configuration is used, with a Pt wire counter electrode and a RHE reference electrode. Inside the cell, the electrode is gently pushed against the CaF_2 prism to carry out SFG measurements in a thin layer configuration.

Electrochemical measurements were performed with an AMEL 5000 programmable potentiostat. The reference electrode was an RHE, all potentials are reported on the RHE scale. A scan rate of 0.05 V s^{-1} has been employed in voltammetric experiments.

2.4. DFT calculations

The simulation of the geometrical and vibrational properties of ethanol and some common electro-oxidation products has been carried out by quantum chemical computations in the framework of the Density Functional Theory (DFT) – as implemented in the Gaussian 03 package [13], with the B3LYP hybrid functional and basis set 6-311+ and Lan2DZ. The vibrational frequency values computed by DFT have been rescaled according to [14]. Following the approach of [15–17] for our first-approximation data interpretation, we simulated the chemisorption process by attaching one Pt atom to the relevant moiety.

3. Results and discussion

3.1. Cyclic voltammetry

In Fig. 1A we report the cyclic voltammograms obtained from a bare WC electrode immersed in a 0.1 M $HClO_4$ solution, in the absence and in the presence of 0.1 M ethanol. The voltammograms were recorded between −0.0 and 1.2 V. We can note that: (i) the oxidation of WC takes place at potentials more anodic than 0.9 V; (ii) a region of hydrogen adsorption is not clearly defined; (iii) the curves recorded in the absence and in the presence of ethanol are very similar. We can conclude that the bare WC electrode does not exhibit any appreciable electrocatalytic behaviour vs. ethanol.

The cyclic voltammetry measurements performed at the same electrode, modified with Pt-black are shown in Fig. 1B (0.1 M $HClO_4$) and 1C (0.1 M $HClO_4$ + 0.1 M EtOH). When the functionalised electrode is immersed in the solution containing only 0.1 M $HClO_4$ (Fig. 1B), we observe a voltammetric behaviour that is very similar to that of a Pt electrode in acidic solution, in terms of hydrogen evolution and Pt oxidation. Moreover, a Tafel-type current due to the oxidation of the WC substrate is observed at potentials more anodic than 1.05 V. In the case of 0.1 M $HClO_4$ + 0.1 M EtOH solution (Fig. 1C), two peaks were observed in the anodic scan, around 0.6 and 0.85 V. According to the interpretation provided in [18], these peaks can be related to ethanol oxidation by: (i) OH_{ads} onto a Pt(I) intermediate state and (ii) PtO, respectively. We can thus conclude that the behaviour of the WC-Pt system, in the relevant potential range, shows the essential characteristics of Pt-based electrodes.

3.2. SFG

SFG experiments were performed with the electrode prepared as described in Section 2.1, in contact with a solution of composition: 0.1 M EtOH, 0.1 M $HClO_4$.

Notwithstanding differences in relative intensities and occasional dips in SFG signal due to imperfect synchronization of the visible and the free-electron lasers, all the SFG spectra exhibit a two-resonance structure, with one peak at ca. 1330 cm^{-1} and a second peak centred either at ca. 1340 or ca. 1345 cm^{-1} (see below for details). SFG spectra were thus fitted with a two-resonance version of the model proposed in [19]. According to this model, the SFG intensity I_{SFG} is: $I_{SFG} \propto |\chi^{(2)}|^2$, where $\chi^{(2)}$ is the complex second-order non-linear susceptibility that, in the present case, can be written as:

$$\chi^{(2)} = a + ib + \frac{A_1}{(\omega - \omega_1) + i\Gamma_1} + \frac{A_2}{(\omega - \omega_2) + i\Gamma_2}$$

where a, b are the real and imaginary parts of the non-resonant contribution, $\omega_{1,2}$ are the resonance frequencies, $A_{1,2}$ are the resonator strengths and $\Gamma_{1,2}$ are the damping coefficients. The extremely high parameter correlation as well as the complexity of the inverse problem discourages quantitative use of the fit parameters different from the resonance frequencies [20].

3.2.1. Potential-dependent SFG spectroscopy

A sequence of SFG spectra was acquired between 0.65 and −1.35 V, by shifting the potential towards cathodic values by steps of 0.25 V each (Fig. 2). Apart from the initial spectrum, that was obtained by pre-polarising the electrode at 0.65 V for 1 h, the potential was set at the desired value just before the acquisition of a spectrum that typically took 20 min. This range spans

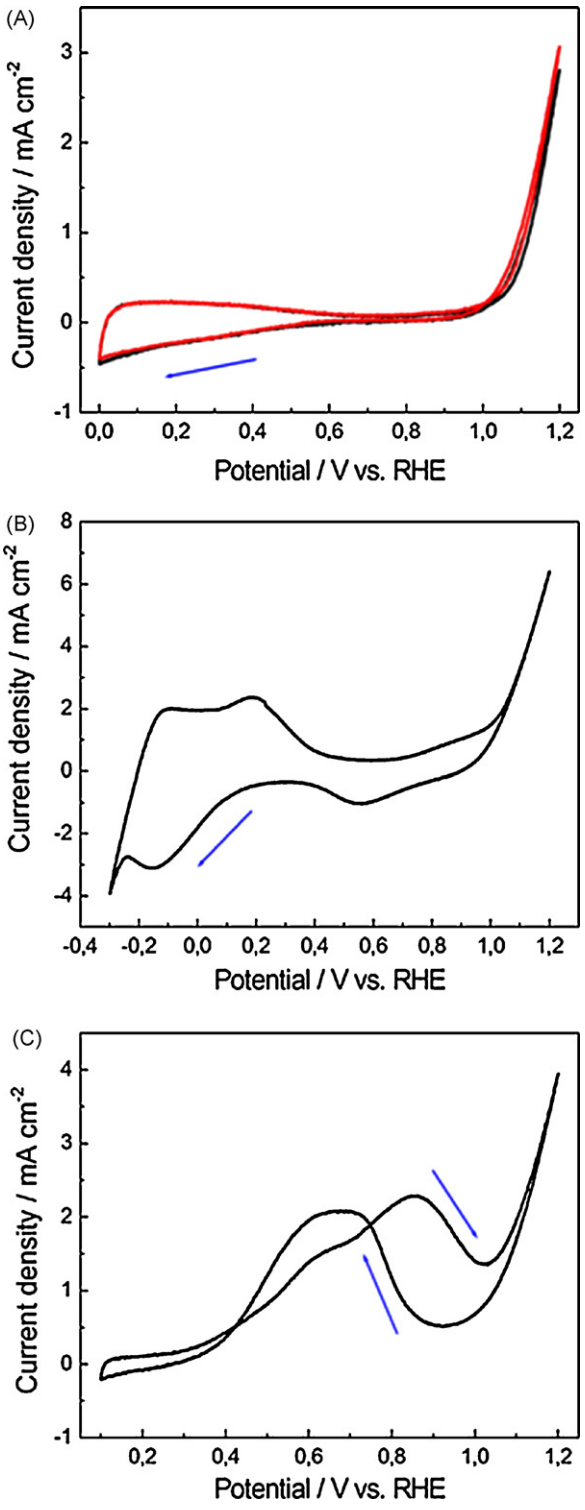

Fig. 1. (A) Cyclic voltammograms obtained with a WC electrode in contact with 0.1 M $HClO_4$ (black line) and 0.1 M $HClO_4$ + 0.1 M CH_3CH_2OH (red line) solutions. (B) Cyclic voltammograms obtained with a WC-supported Pt-black electrode in contact with a 0.1 M $HClO_4$ solution. (C) Cyclic voltammograms obtained with a WC-supported Pt in contact with a 0.1 M $HClO_4$ + 0.1 M CH_3CH_2OH solution. In all cases, the scan rate is 0.05 mV s^{-1}. (For interpretation of the references to colour in this figure legend, the reader is referred to the web version of the article.)

ethanol oxidation at cathodically protected WC and cathodic desorption of oxidation products. At all potentials investigated a complex spectral pattern is found, with a dominating band at ca. 1340–1345 cm^{-1}, more prominent in the range 0.65 to −0.1 V. This band is accompanied by a smaller resonance at ca. 1330 cm^{-1}; at

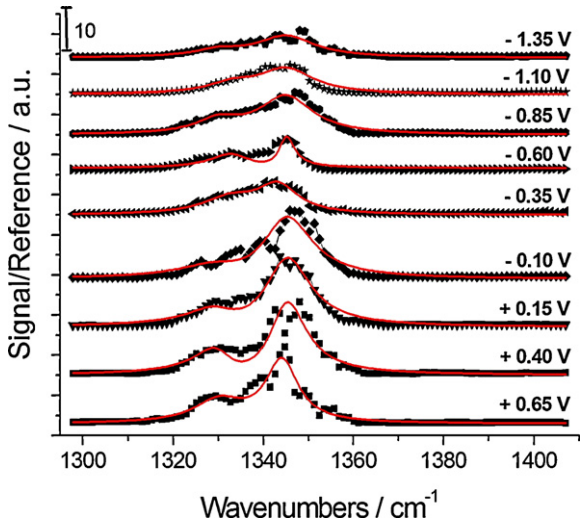

Fig. 2. Sequence of SFG spectra measured in the range 0.65 to −1.35 V_{RHE} on a WC/Pt-black electrode in contact with a 0.1 M $HClO_4$ + 0.1 M CH_3CH_2OH solution.

the higher cathodic potentials investigated, the intensities of all the bands tend to vanish, probably owing to cathodic desorption.

Even though an assignment of each band based on strictly mechanistic considerations is beyond the scope of this work – chiefly addressing spectroscopic aspects – and the intrinsic instrumental limitation of the free-electron laser – related to the linear electron accelerator and undulator properties – render it impossible to explore a wider range of IR frequencies in search of other adsorbate resonances, we tentatively identified the nature of SFG resonances with the support of related literature and original DFT calculations of the vibrational modes of ethanol and of its main reaction products that have been reported to be obtained by electro-oxidation. Even though the literature on the mechanistic details of electrochemical ethanol oxidation is not unanimous and the problem is strictly material-dependent, it is generally accepted that ethanol on Pt undergoes oxidation via parallel pathways (see, e.g. [21–23] and references contained therein), and can occur via the formation of adsorbates containing 2 or 1 C atoms. The mechanism of partial oxidation of ethanol to acetaldehyde, acetic acid and CO is still unclear; in particular, it has not been clarified yet whether it occurs through the direct oxidation of ethanol to acetic acid or via adsorbed acetaldehyde (i.e. [24]). The complete oxidation of ethanol is, of course, achieved via the breaking of the C–C bond and the complete oxidation of the two fragments containing 1 C atom each eventually to CO_2 [25]. Regardless of the details of the reaction mechanism, CO_2, acetaldehyde and acetic acid are unanimously reported as the main products of ethanol oxidation ([26,27] and therein contained references), their relative yields depending on the initial concentration of ethanol [23]. Besides CO_{ads}, other residues deriving from the oxidative adsorption of ethanol were identified: $Pt–OCH_2–CH_3$, $(Pt)_2{=}COHCH_3$, $PtCOCH_3$ and $Pt_2CO_2CH_3$ ([21] and references therein contained).

On the basis of the SFG results reported in Fig. 2 and of our DFT computations, we can conclude that:

(i) The band at ca. 1330 cm^{-1} can be assigned to the O=C=O asymmetric stretching of adsorbed acetate (DFT computations yield the band position 1324 cm^{-1}; this mode is SFG active, since the computed ratio of the IR to Raman intensities is I_{IR}/I_{Raman} = 1.006). According to [28], the acetate moiety is adsorbed perpendicularly to the Pt surface through the oxygen atoms in the bridge configuration.

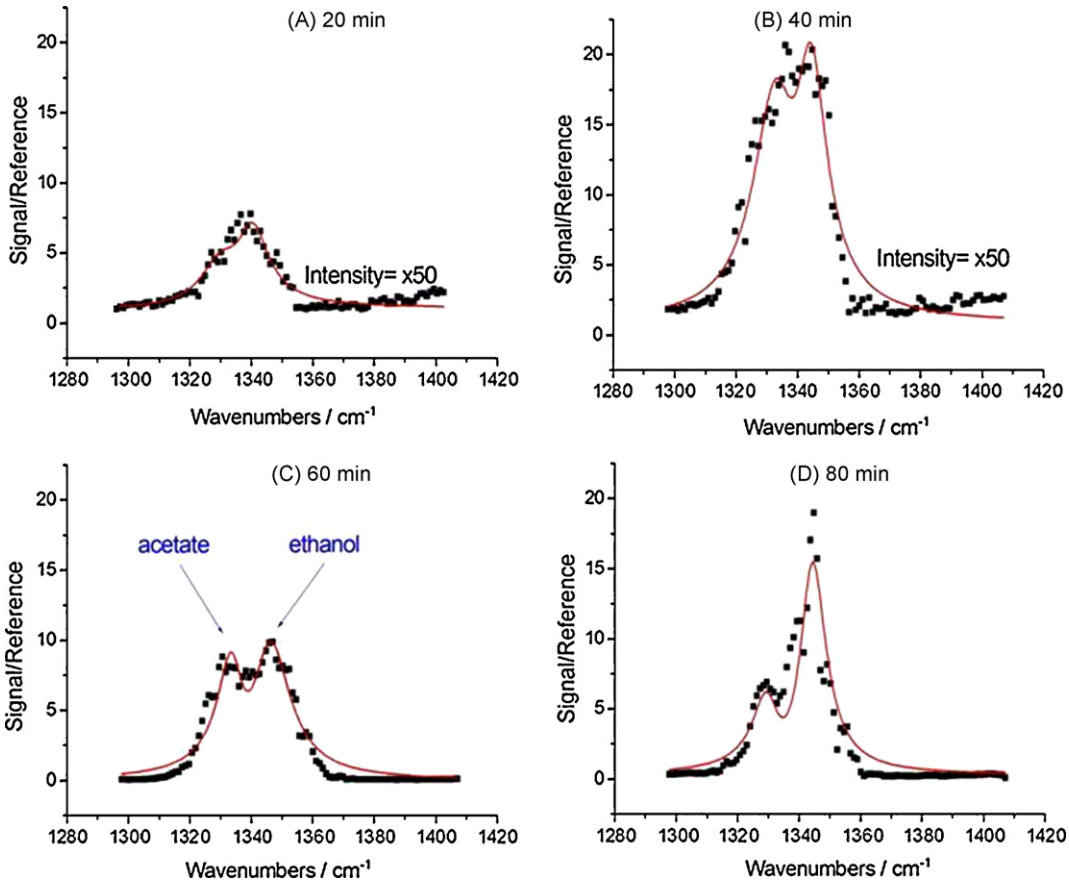

Fig. 3. Sequence of four successive SFG spectra taken each after 20 min of electrochemical polarisation at 0.65 V_{RHE} on a WC/Pt-black electrode in contact with a 0.1 M $HClO_4$ + 0.1 M CH_3CH_2OH solution.

(ii) The bands at 1340/1345 cm^{-1} can be assigned to the OH and CH wagging combination of adsorbed ethanol via the C atom and to the CH_2 wagging of adsorbed ethanol via the O atom [21] (DFT computations yield the band positions 1338/1342 cm^{-1}). These bands can be regarded as a fingerprint of the adsorption of undissociated ethanol, in fact: (i) combined O–H and C–H wagging in ethanol adsorbed via the C atom yield a computed band at 1338 cm^{-1} (SFG active, since $I_{IR}/I_{Raman} = 2.875$); CH_2 wagging in ethanol adsorbed via the O atom yields a computed band at 1342 cm^{-1} (SFG active, since $I_{IR}/I_{Raman} = 2.555$).

Adsorbed acetaldehyde – often reported as a typical oxidation intermediate – exhibits calculated bands below 1124 and above 1400 cm^{-1} that do not match with the spectral range accessible to our experimental setup.

3.2.2. Time-dependence of SFG spectra

By applying polarisation sequences different from the potential staircase used for the acquisition of the set of spectra shown in Fig. 2 (see Section 3.2.1 for details), it was found that SFG spectral patterns exhibit a time-dependent behaviour, likely related to reactive adsorption kinetics.

In particular, we have studied the following polarisation programs: (i) potentiostatic ethanol oxidation at 0.65 V, where WC is cathodically protected (Fig. 3); (ii) the potential is stepped from 0.65 V into the cathodic desorption range (0.0 and −0.5 V, Fig. 4); (iii) the potential is stepped from 0.65 V to more anodic conditions, in order to reach the WC oxidation range (0.9 V, Fig. 5).

3.2.2.1. Ethanol oxidation at 0.65 V. A set of time-dependent measurements, starting from open-circuit conditions, each after 20 min of electrochemical polarisation at 0.65 V – in the ethanol oxidation range, but well cathodic with respect to WC oxidation – is shown in Fig. 3. During the first two acquisitions (Fig. 3A and B, corresponding to 20 and 40 min of electrochemical polarisation, respectively),

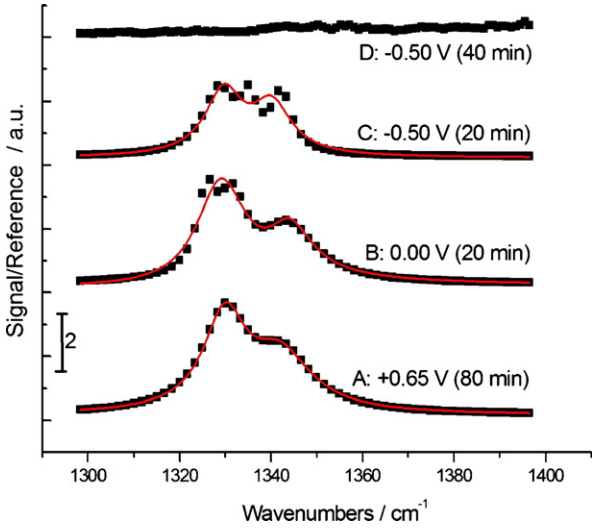

Fig. 4. Sequence of SFG spectra measured sequentially (according to alphabetical ordering) in the range 0.65 to −0.50 V_{RHE} on a WC/Pt-black electrode in contact with a 0.1 M $HClO_4$ + 0.1 M CH_3CH_2OH, recorded after the indicated polarisation times.

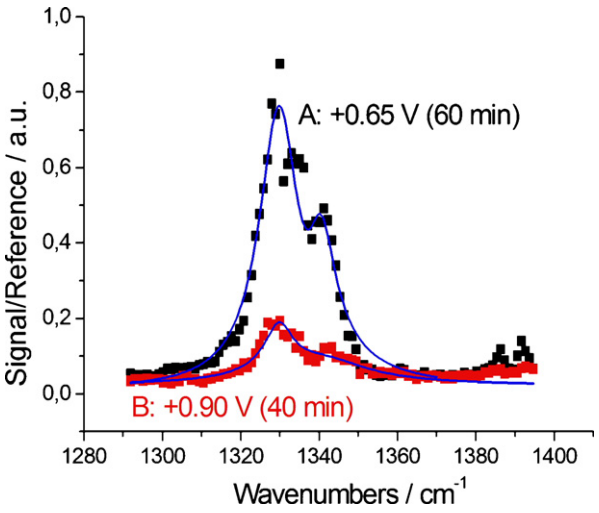

Fig. 5. SFG spectra measured sequentially (according to alphabetical ordering) at 0.65 and 0.90 V_{RHE} on a WC/Pt-black electrode in contact with a 0.1 M $HClO_4$ + 0.1 M CH_3CH_2OH, recorded after the indicated polarisation times.

a broad band centred at around 1340 cm^{-1} was observed. As a function of electrochemical polarisation time, a remarkable resonance developed and well-defined peaks built up at ca. 1330 and ca. 1345 cm^{-1} (Fig. 3C and D). In particular, the intensity of the peak at ca. 1345 cm^{-1} drastically increased after 60 min.

The time-dependent evolution of the spectral pattern can be described in terms of progressive change from a spectral pattern dominated by adsorbed acetate towards features corresponding to ethanol adsorption.

3.2.2.2. Cathodic desorption. Cathodic desorption was studied by first setting oxidative adsorption conditions at 0.65 V for 80 min and then stepping into the cathodic desorption range at two different potentials: 0.0 and −0.5 V (Fig. 4). In Fig. 4A the spectrum obtained at 0.65 V is very similar – though not identical, owing to the time-dependent behaviour highlighted in Section 3.2.2.1 – to the bands shown in Fig. 3. At 0.0 V (Fig. 4B) we observed a slight decrease of the signal, accompanied by minor changes of the relative intensity of the bands. At −0.5 V, further changes in relative intensities (Fig. 4C) and notable, progressive loss of signal are measured (Fig. 4D). It is worth noting that in Fig. 2, measured holding the electrode at the relevant potentials for times shorter that in the experiments reported in Fig. 4, a relatively well-defined resonance could still be measured at even higher cathodic potentials (−0.85 and −1.35 V).

3.2.2.3. Anodic desorption. After completion of the cathodic desorption experiment described in Section 3.2.2.2, re-adsorption is performed at 0.65 V (Fig. 5A), yielding spectra that exhibit the two typical resonances. The potential was then set at 0.9 V (Fig. 5B), where WC corrosion takes place along with ethanol oxidation and, as a result, the signal intensity was notably lowered.

4. Conclusions

In this paper we describe an in situ sum-frequency generation (SFG) spectroelectrochemical investigation of the electro-oxidation of ethanol at Pt-black supported on WC. Two types of resonances were observed at 1330 (O=C=O asymmetric stretching in acetate), 1340/1345 cm^{-1} (OH and CH wagging combination of ethanol adsorbed via the C atom and CH_2 wagging of ethanol adsorbed via O atom). These resonances correspond to the reagent and the intermediate: the type of ethanol adsorption mode and the relative intensities are a complex function of applied potential and polarisation time. In situ SFG thus gives an unequivocal proof of the coadsorption of acetate and ethanol. Cathodic and anodic desorption processes have been highlighted, the latter probably controlled by WC corrosion. The spectral patterns observed are strongly irreversible and – in particular at 0.65 V where ethanol oxidation goes on with cathodically protected WC – it was found that ethanol tends to dominate over acetate for prolonged oxidation times.

Acknowledgement

Collaboration with experimental work and data analysis is gratefully acknowledged to Caterina Manera, MSc.

References

[1] D.R. McIntyre, G.T. Burstein, A. Vossen, J. Power Sources 107 (2002) 67–73.
[2] G. Lu, J.S. Cooper, P.J. McGinn, J. Power Sources 161 (2006) 106–114.
[3] C.D.A. Brady, E.J. Rees, G.T. Burstein, J. Power Sources 179 (2008) 17–26.
[4] H. Chhina, S. Campbell, O. Kesler, J. Power Sources 164 (2007) 431–440.
[5] F.P. Hu, P.K. Shen, J. Power Sources 173 (2007) 877–881.
[6] C. Bianchini, P.K. Shen, Chem. Rev. 109 (2009) 4183–4206.
[7] H. Meng, P.K. Shen, Chem. Commun. (2005) 4408–4410.
[8] Z. Hu, M. Wu, Z. Wei, Sh. Song, P.K. Shen, J. Power Sources 166 (2007) 458–461.
[9] M. Nie, H. Tang, Z. Wei, S.P. Jiang, P.K. Shen, Electrochem. Commun. 9 (2007) 2375–2379.
[10] F. Hu, G. Cui, Z. Wei, P.K. Shen, Electrochem. Commun. 10 (2008) 1303–1306.
[11] H.R. Colón-Mercado, B.N. Popov, J. Power Sources 155 (2006) 253–263.
[12] C. Humbert, B. Busson, C. Six, A. Gayral, M. Gruselle, F. Villain, A. Tadjeddine, J. Electroanal. Chem. 621 (2008) 314–321.
[13] M.J. Frisch, G.W. Trucks, H.B. Schlegel, G.E. Scuseria, M.A. Robb, J. Cheeseman, J.A. Montgomery Jr., T. Vreven, K.N. Kudin, J.C. Burant, J.M. Millam, S.S. Iyengar, J. Tomasi, V. Barone, B. Mennucci, M. Cossi, G. Scalmani, N. Rega, G.A. Petersson, H. Nakatsuji, M. Hada, M. Ehara, K. Toyota, R. Fukuda, J. Hasegawa, M. Ishida, T. Nakajima, Y. Honda, O. Kitao, H. Nakai, M. Klene, X. Li, J.E. Knox, H.P. Hratchian, J.B. Cross, V. Bakken, C. Adamo, J. Jaramillo, R. Gomperts, R.E. Stratmann, O. Yazyev, A.J. Austin, R. Cammi, C. Pomelli, J.W. Ochterski, P.Y. Ayala, K. Morokuma, G.A. Voth, P. Salvador, J.J. Dannenberg, V.G. Zakrzewski, S. Dapprich, A.D. Daniels, M.C. Strain, O. Farkas, D.K. Malick, A.D. Rabuck, K. Raghavachari, J.B. Foresman, J.V. Ortiz, Q. Cui, A.G. Baboul, S. Clifford, J. Cioslowski, B.B. Stefanov, G. Liu, A. Liashenko, P. Piskorz, I. Komaromi, R.L. Martin, D.J. Fox, T. Keith, M.A. Al-Laham, C.Y. Peng, A. Nanayakkara, M. Challacombe, P.M.W. Gill, B. Johnson, W. Chen, M.W. Wong, C. Gonzalez, J.A. Pople, Gaussian 03, Gaussian, Inc., Pittsburgh, PA, 2003.
[14] J.B. Foresman, Æ. Frisch, Exploring Chemistry with Electronic Structure Methods, Gaussian Inc., Pittsburgh, 1996, pp. 64 and 90.
[15] M. Tadjeddine, J.P. Flament, A. Tadjeddine, J. Electroanal. Chem. 408 (1996) 237–242.
[16] M. Tadjeddine, J.P. Flament, Chem. Phys. 240 (1999) 39–50.
[17] B. Bozzini, L. D'Urzo, C. Mele, V. Romanello, J. Phys. Chem. C 112 (2008) 6352–6358.
[18] S.S. Gupta, J. Datta, J. Electroanal. Chem. 594 (2006) 65–72.
[19] A. Tadjeddine, A. Le, Rille, in: A. Wieckowski (Ed.), Interfacial Electrochemistry, Dekker, NY, 1999, pp. 317–343.
[20] I. Sgura, B. Bozzini, Int. J. Non-linear Mech. 40 (2005) 557–570.
[21] M.H. Shao, R.R. Adzic, Electrochim. Acta 53 (2008) 2963–2971.
[22] B. BittinsCattaneo, S. Wilhelm, H.W. Bushmann, W. Vielstich, Ber. Bunsenges, Phys. Chem. 92 (1988) 1210–1218.
[23] G.A. Camara, T. Iwasita, J. Electroanal. Chem. 578 (2005) 315–321.
[24] S.Q. Song, et al., Int. J. Hydrogen Energy 30 (2005) 995–1001.
[25] K. Bergamaski, E.R. Gonzalez, F.C. Nart, Electrochim. Acta 53 (2008) 4396–4406.
[26] E. Antolini, J. Power Sources 170 (2007) 1–12.
[27] T. Iwasita, B. Rasch, E. Cattaneo, W. Vielstich, Electrochim. Acta 34 (1989) 1073–1079.
[28] X.H. Xia, H.-D. Liess, T. Iwasita, J. Electroanal. Chem. 437 (1997) 233–240.